THE JOURNAL OF PHYSICAL CHEMISTRY Letters

Letter

Cite This: J. Phys. Chem. Lett. 2019, 10, 2196−2201

pubs.acs.org/JPCL

Bright Quantum Dot Light-Emitting Diodes Enabled by Imprinted Speckle Image Holography Nanostructures

Hao Chen,[†,‡,⊥] Ziqian He,[‡,⊥] Dandan Zhang,[*,†,§] Caicai Zhang,[†,∥] Yi Ding,[†,∥] Laurene Tetard,[†,∥] Shin-Tson Wu,[*,‡] and Yajie Dong[*,†,‡,∥]

[†]NanoScience Technology Center, University of Central Florida, Orlando, Florida 32826, United States

[‡]College of Optics and Photonics, University of Central Florida, Orlando, Florida 32816, United States

[§]Institute of Functional Nano & Soft Materials (FUNSOM), Soochow University, Suzhou 215123, P. R. China

[∥]Department of Materials Science & Engineering, University of Central Florida, Orlando, Florida 32816, United States

Supporting Information

ABSTRACT: Super-bright all-solution-processed quantum dot light-emitting diodes (QLEDs) with an inverted structure are achieved by imprinting speckle image holography (SIH) structures inside the devices. QLEDs with imprinted random grating structures can reach a luminance of up to 146 000 Cd/m^2 at driving voltage of 8 V, which is 1.76 times higher than the value of control devices with planar architecture, setting a new brightness record for all-solution-processed inverted red QLEDs. The luminous power efficiency and external quantum efficiency of the QLEDs with imprinted structures are 1.8 and 1.65 times higher to those of the control devices, respectively. Further optical simulation results reveal that not only can the structure help extract the trapped internal photon energy but also the mechanical pressure during the imprinting process plays a crucial role in improving the device performance.

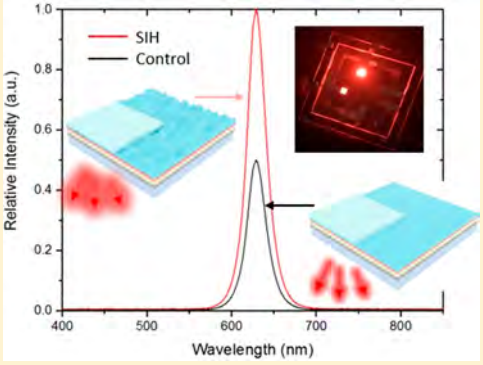

Quantum dot light-emitting diodes (QLEDs) have attracted intense attention since their inception due to their unique properties, such as tunable emitting wavelengths, saturated color, solution processability, and so on.[1−5] The past decades have witnessed tremendous progress for QLED development. Until now, QLEDs, through a low-cost solution-processing pathway, have already been demonstrated to have comparable efficiency to state-of-the-art organic light-emitting diode (OLED) and are being generally regarded as one of the most promising candidates for next-generation display technology.[6−16] Display giants, like BOE and TCL, have already demonstrated their prototype QLED panels.[17,18] However, the lifetime of QLEDs, especially for blue color, remains a limiting factor for their immediate adoption into the real market.[2,19]

Beyond the application in display, the potential to achieve high brightness renders QLEDs the capacity to be employed for photomedical applications, where high output power (>20 000 cd/m^2) and narrow emitting spectra within the deep-red range (620−670 nm) are highly desired.[20] Considering the promise of QLEDs to be low-cost, wearable, disposable light-emitting bandage products, photomedicine can be the niche in which QLEDs can perfectly fit without worrying about the lifetime issue. Recently, our group has demonstrated preliminary results of ultrabright QLED-based photomedicine[21] and successfully developed all-solution-processed inverted QLEDs to lower the cost.[22] Nevertheless, higher luminance, all-solution-processed QLEDs are still preferred for more economical and efficient photomedical treatment.

Although existing QLEDs can reach a very high internal quantum efficiency (IQE > 90%),[7,10,17] the external quantum efficiency (EQE) is limited to ∼20%. A large fraction of light (80%) is lost due to the different mechanisms that occur inside the device including the substrate mode loss, indium tin oxide (ITO)/organic waveguide mode loss, and surface plasmon polariton (SPP) mode loss.[23] To extract out the light lost inside the devices more efficiently, various internal and external strategies can be employed.[24,25]

Recently, holographic metasurfaces have emerged as an effective strategy to engineer photons within subwavelength interaction lengths and have been applied in amplitude modulators,[26] 3D plasmonic holographic displays,[27,28] highly efficient polarization converters,[29] data storage,[30] optical tweezers,[31] and beam reshaping.[32] Moreover, holographic metasurfaces have been reported to provide outstanding light extraction performance in OLEDs.[33] Compared with other light extraction strategies, the holographic metasurfaces can be relatively easily generated. With nanoimprint lithography, the pattern transformation to device layers can be readily achieved and is compatible with all-solution processing. The near-field and far-field properties of the devices can also be manipulated

Received: February 20, 2019
Accepted: March 27, 2019
Published: March 27, 2019

DOI: 10.1021/acs.jpclett.9b00499
J. Phys. Chem. Lett. 2019, 10, 2196−2201

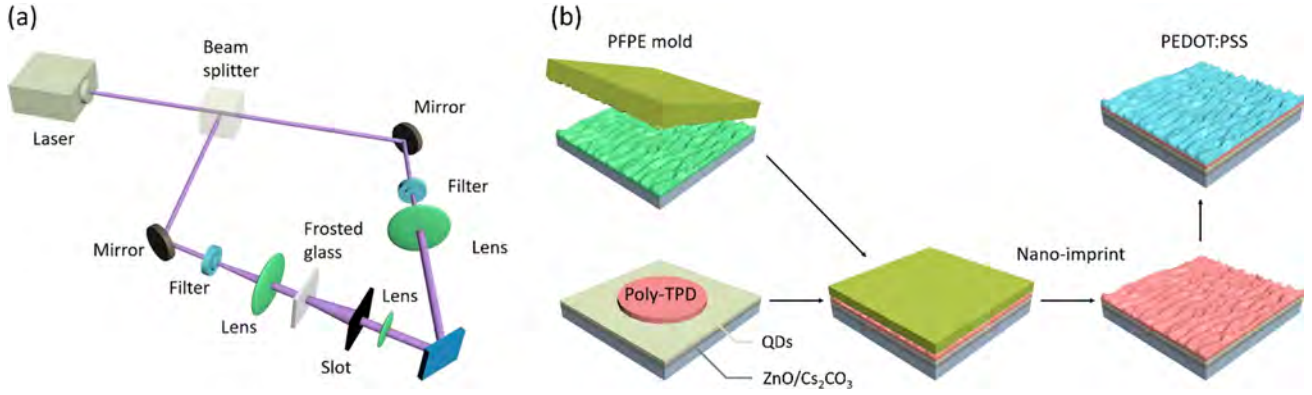

Figure 1. Schematic illustration of the fabrication process of (a) SIH nanostructures and (b) red QLEDs with imprinted SIH nanostructures. In the SIH-QLED fabrication, a PFPE stamp was cast from the SIH sample and imprinted onto the poly-TPD layer. The rest of the steps followed the all-solution processing from a previous report.[22]

by introducing different holograms. A similar enhancement can be expected for QLEDs. However, investigations on holographic metasurface-enhanced QLEDs for light extraction are still lacking.

In this Letter, we demonstrate a simple approach to extract the trapped photons out of QLED devices without changing the angle-dependent emission properties. By transferring speckle image holographic (SIH) metasurface structure onto the device layers via an imprinting method, red-emitting QLEDs with a luminance of 146 000 Cd/m^2 at 8 V can be achieved, which is 1.76 times higher than the value of control devices with a regular structure. To the best of our knowledge, it is a new brightness record for all-solution-processed inverted red QLEDs. The luminous power efficiency and EQE of the QLEDs with SIH structure are 1.8 and 1.65 times those of the control devices, respectively. Further simulation results indicate that the imprinting method can not only extract the trapped photons for a higher efficiency but also improve the device performance through an imprinting-induced film-compression mechanism.

Figure 1a illustrates the fabrication process of SIH structures by an interference exposure method. Specifically, photoresist PZJ390PR (Suzhou Ruihong) was first spin-coated onto a precleaned glass substrate with a thickness of 800 nm and then baked for 1 min at 120 °C. To expose, a He−Cd laser beam (441 nm) was separated into two beams with approximately equal intensities by a nonpolarizing beam splitter, and the two beams were then amplified by two neutral-density filters, respectively. The speckle object wave was generated by inserting a frosted glass and a rectangular slot in one path and imaged onto the photoresist. Meanwhile, the reference wave was collimated onto the photoresist, with an angle of 60° to the object wave. After exposing for 45 s, the sample was developed in NaOH (0.4%) solutions for 10 s and dried by an electric blow drier.

Figure 1b shows the entire process for soft mold preparation and the structured QLED fabrication. To fabricate the SIH-nanostructured perfluoropolyether (PFPE) soft mold, a photocurable liquid PFPE (α,Ω-functionalized dimethacrylate) precursor solution consisting of 1000 g mol^{-1} PPFP and a photoinitiator, 2,2-diethoxyacetophenone, was poured onto the surface of a prefabricated SIH photoresist template and then embossed under a constant pressure of 1.2 bar with UV illumination at a wavelength of 395 nm at 500 mJ cm^{-2} for 15 s. Subsequently, the PFPE soft mold was peeled off of the photoresist. On the contrary, the structure of our QLED devices consists of layers including ITO/ZnO nanoparticles and the Cs_2CO_3 mixture layer (~10 nm)/CdSe−ZnS−CdZnS core−shell−shell quantum dots (QDs) (~20 nm)/poly(*N*,*N*9-bis(4-butylphenyl)-*N*,*N*9-bis(phenyl)-benzidine) (poly-TPD) (~40 nm)/poly(ethylenedioxythiophene):polystyrenesulfonate (PEDOT:PSS) (~50 nm)/Al anode (~100 nm). These inverted red QLED devices were fabricated by an all-solution process, as described in a previous report,[22] and the prepared random grating structures were introduced onto the poly-TPD layer by soft nanoimprint lithography, as depicted in Figure 1b. (Details of SIH-QLED device fabrication can be found in Supporting Note 1.) This layer was chosen as the patterning layer because it has reasonable thickness and is easy to detach from the mold.

It is worth mentioning that ZnO nanoparticles and Cs_2CO_3 are both proven to have excellent electron injection capacity in that ZnO nanoparticles (optical properties can be found in Figure S1) have a deep HOMO level of 7.2 eV, which can effectively block hole leakage pathway, whereas thin Cs_2CO_3 film demonstrates a high LUMO level of 2.8 eV. The as-obtained mixture film can take benefits from both materials, providing a low-work-function electron injection layer (EIL) with enhanced hole-blocking effect. In terms of red emission materials, CdSe−ZnS−CdZnS core−shell−shell QDs with a peak wavelength of 625 nm and a narrow full width at half-maximum (fwhm) of 21 nm in solution were applied. (Optical properties can be found in Figure S2.) These giant quantum dots (QDs) with double shells can dramatically suppress Augur recombination, thus rendering the QDs the potential to maintain high luminescence efficiency under high-pump conditions. Poly-TPD and PEDOT:PSS are widely used as hole transport layer (HTL) and hole injection layer (HIL) materials due to their high hole mobility, good energy level, and solution processability. In particular, PEDOT:PSS solution is doped with Triton X-100 by a small ratio of 0.21 wt % to increase the wettability and adhesion at the interface of aqueous PEDOT:PSS/poly-TPD layer, enabling the solution deposition of PEDOT:PSS onto the hydrophobic poly-TPD.[34−36]

The key to improving QLED performance in our case is the SIH nanostructures. The atomic force microscopy (AFM) images (see Supporting Note 2) of the random grating structure on the PFPE mold, poly-TPD, and PEDOT:PSS are shown in Figure 2a−c with depths of 220, 30, and 15 nm,

DOI: 10.1021/acs.jpclett.9b00499
J. Phys. Chem. Lett. 2019, 10, 2196−2201

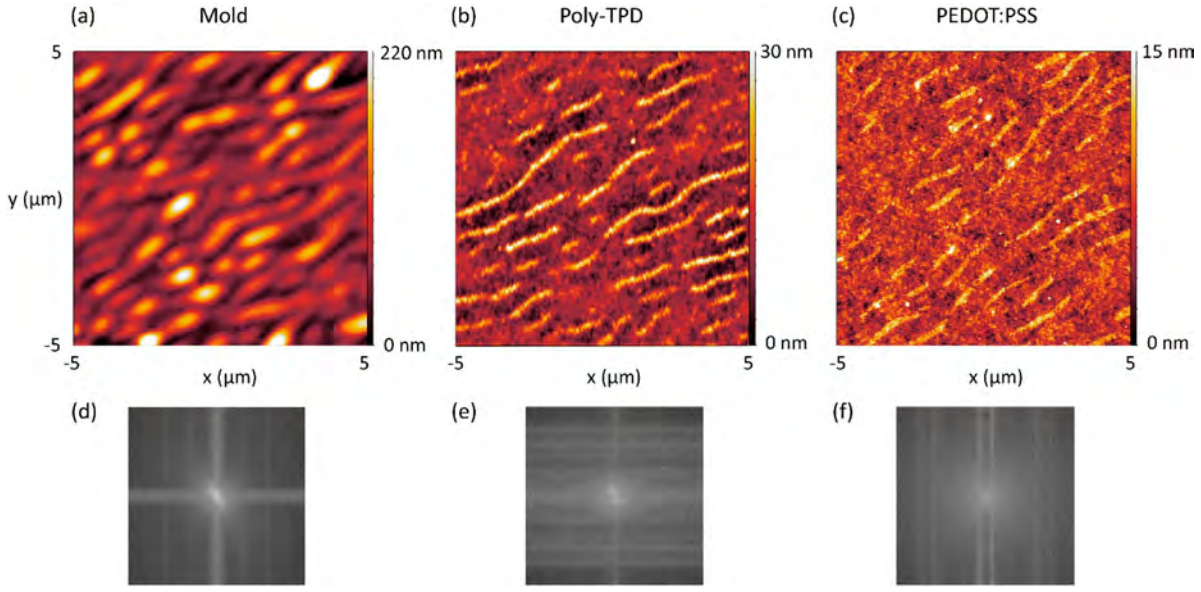

Figure 2. AFM images of (a) the PFPE mold, (b) the patterned poly-TPD layer, and (c) the patterned PEDOT:PSS layer on ITO glass substrates. (d–f) Corresponding fast Fourier transform (FFT) patterns of the AFM images in panels a–c, respectively.

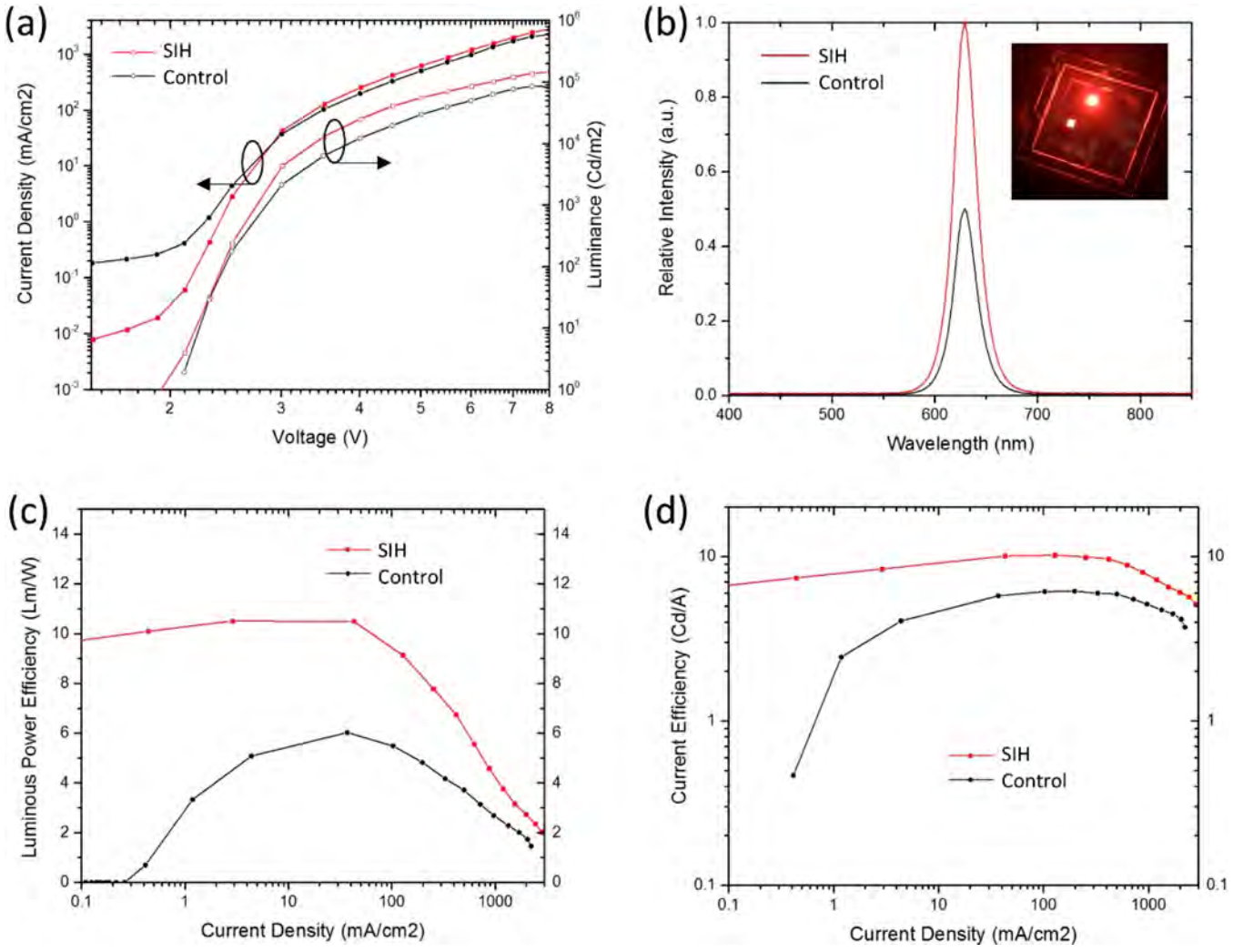

Figure 3. Performance characteristics of red-emitting QLEDs. (a) Current density–luminance–voltage characteristics. (b) Relative EL spectra in the normal direction to the glass substrate at $V = 3$ V. (c) Luminous power efficiency as a function of current density. (d) Current efficiency as a function of current density.

DOI: 10.1021/acs.jpclett.9b00499
J. Phys. Chem. Lett. 2019, 10, 2196–2201

respectively. The nanostructure can be transferred onto the poly-TPD layer using a soft PFPE stamp well but with shallower depths. The patterns are somewhat faded but can still be observed after depositing the PEDOT:PSS layer. To investigate the spatial frequency characteristics, the corresponding fast Fourier transform (FFT) patterns of these AFM images are calculated and exhibited in Figure 2d–f. The random structure exhibits a rich Fourier spectrum of k vectors, which offers broadband angular responses and leads to omnidirectional scattering. Upon imprinting, the k-vector distribution seems to be even more spread out for poly-TPD and PEDOT:PSS layers. This striking feature indicates that our device should form uniform far-field patterns, whereas those with periodic structures will exhibit discrete hot spots/lines in the far field.[33]

Electroluminescence (EL) properties of SIH-QLEDs have been measured and compared with those of planar QLEDs to investigate the functions of the SIH structure. J–L–V results of SIH-QLEDs and control planar QLEDs are shown in Figure 3a (L–J relationship is plotted separately in Figure S3). The imprinted devices exhibit much lower leakage current before devices turn on. This phenomenon can be attributed to the more compact layers induced by external pressure from the imprinting process. A subtle difference for the current density curve can be observed after turning on the devices. The relatively larger contact area for the imprinted layer and the small variation of film thickness might be the reason for the slightly higher current density of SIH-QLEDs, consistent with previous work.[25]

The EL spectrum (as exhibited in Figure 3b) of SIH-QLEDs displays a saturated (fwhm of 25 nm with a peak wavelength of 629 nm) QD emission profile and is slightly red-shifted (4 nm) from the solution photoluminescence measured on the same QD material. This red shift can be attributed to a combination of interdot interactions, which have been previously observed in closely packed QD solids, and to the electric-field-induced Stark effect.[7] The 1931 Commission Internationale de l'Eclairage (CIE) x–y coordinates of our QLEDs are (0.69, 0.31), falling into the deep red range, a region favorable for many photomedicine applications.[20]

It should be highlighted that the SIH-QLEDs with a turn-on voltage of ~2 V can reach a luminance of up to 146 000 Cd/m^2 at just 8 V, whereas the luminance of planar devices is 83 000 Cd/m^2 under the same driving condition, corresponding to a 1.8 times higher luminous power efficiency and a 1.65 times higher current efficiency (which is propotional to EQE), as demonstrated in Figure 3c,d. The peak luminance of SIH-QLEDs, to the best of our knowledge, is a record luminance for existing all-solution-processed inverted red QLEDs. It is worth mentioning that whereas the nanostructures are random, we have consistently observed a similar enhancement effect in all three batches of devices fabricated at different times, with different control baseline device performances. The enhancement has been listed in Table S1.

Angle-dependent luminescence and color shift measurement results are presented in Figure 4. The control device with a planar structure exhibits ideal Lambertian distribution, whereas the imprinted QLEDs illustrate a modified profile with an almost constant enhancement factor within a wide viewing angle ranging from −60 to 60°, indicating that the output light scattered by the SIH structure has been well modulated. Moreover, thanks to the narrow emission spectra of QDs and the wavelength-independent enhancement of the SIH

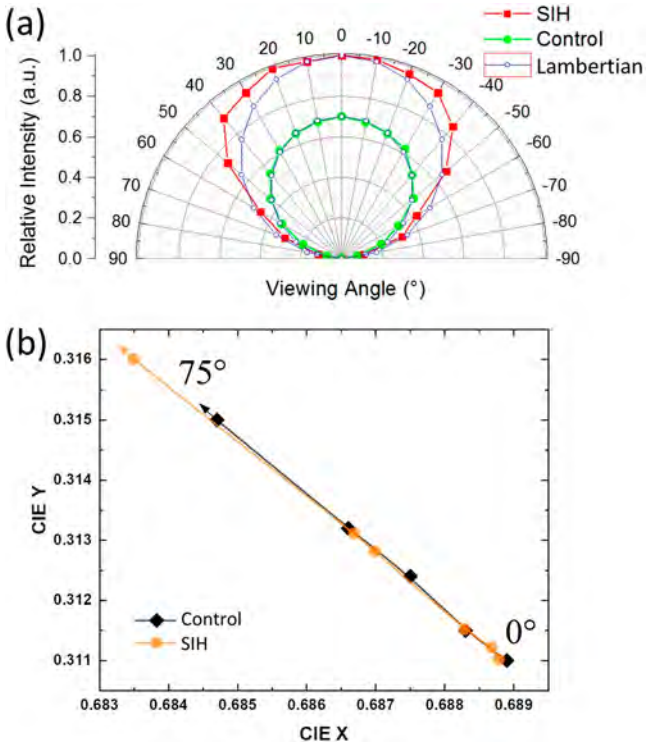

Figure 4. (a) Measured relative angular luminance for SIH-QLEDs and control devices. Ideal Lambertian distribution is also provided as reference. (b) Measured angular color shift in the CIE 1931 color space for SIH-QLEDs and control devices, where arrows indicate the shift of viewing angle from 0 to 75° in steps of 15°.

structure, almost no difference in color shift has been observed for SIH-QLEDs when compared with control devices, as depicted in Figure 4b. Again, this assures the small impact of the random grating structure on angular emission properties.

Previously, work has been done to investigate the near-field and far-field radiation property differences between grating- and SIH-imprinted OLEDs.[33] Because of the randomness of our SIH structures, the radiation performance should be similar. Here, to reveal the effectiveness of light extraction induced by the SIH structure, the finite-difference time-domain (FDTD) method (see Supporting Note 3) was applied to simulate the energy distribution to different modes for both SIH-QLEDs and planar QLEDs. Figure 5 plots the ratio of each mode in accordance with the poly-TPD thickness. As can be noticed, the SIH structure can effectively decrease the energy trapped in the waveguide mode through random scattering-induced outcoupling. As a result, the energy distributed to air and substrate modes is readily increased. For an SIH-QLED device with 40 nm poly-TPD, the energy ratio of the air mode is ~26%. If external outcoupling structures are further applied, then the total EQE can reach as high as 47%. It is worth mentioning that for devices with 40 nm poly-TPD, the enhancement of the air mode (compare SIH-OLED with planar OLED) is ~40%, which is less than that observed in the experiment (65%). We ascribed this difference to an imprinting-induced film-compression mechanism. The presence of the mechanical pressure during the imprinting process may lead to more compact films, which could result in less leakage current and increased coulomb interaction between holes and electrons within the interface between the QD layer and EIL/HTL layers, leading to a better

DOI: 10.1021/acs.jpclett.9b00499
J. Phys. Chem. Lett. 2019, 10, 2196–2201

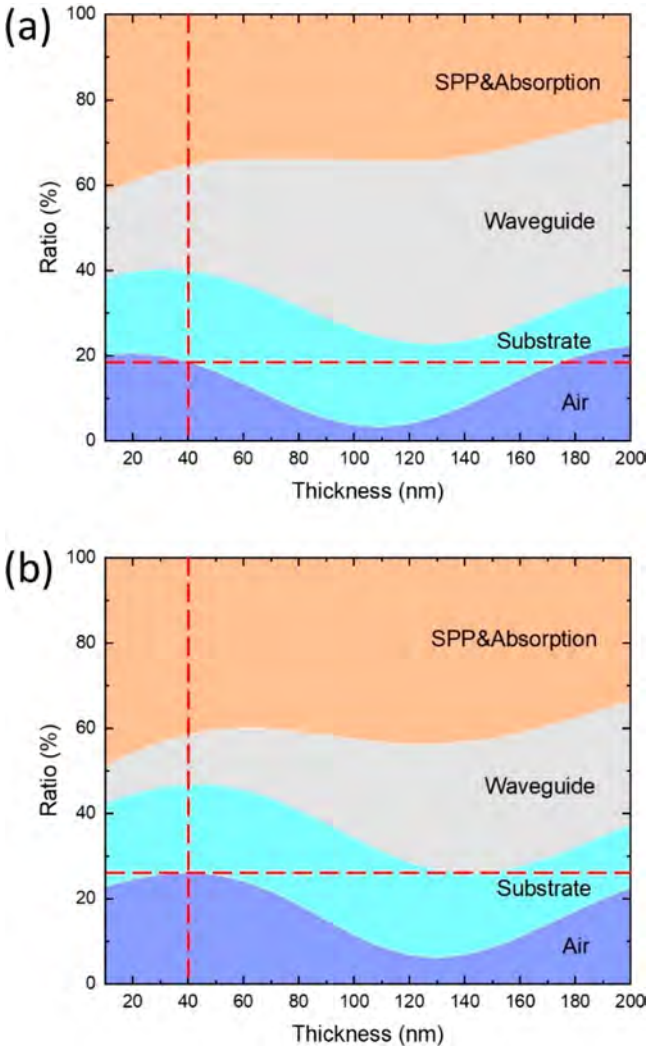

Figure 5. Simulation results of the energy distribution to different optical modes as a function of poly-TPD thickness for (a) planar structure QLEDs and (b) SIH-QLEDs.

EL performance.[37,38] The electrical property improvement can be noticed in Figure 3a. It turns out that the SIH device exhibited a lower current leakage below threshold voltage. The larger parallel resistance (see Supporting Note 4) may be related to pressure-induced surface passivation.

In summary, a simple method to extract the trapped photons out of QLED devices was demonstrated. Through transferring SIH metasurface structure onto the device layers via an imprinting method, red-emitting QLEDs with a luminance of 146 000 Cd/m^2 at a driving voltage of 8 V were achieved, which is 1.76 times higher than the value of control devices with a planar structure, setting a new brightness record for all-solution-processed inverted red QLEDs. The luminous power efficiency and EQE of the SIH-QLEDs are 1.8 and 1.65 times those of the control devices with a standard architecture, respectively. Moreover, the introduction of the SIH structure proved to have a negligible effect on angular-dependent optical properties and the emitting spectrum. Further simulation results indicate that the benefits of the imprinting method are two-fold. It not only helps extract the trapped photons via the SIH structure but also improves the device performance through an imprinting-induced film-compression mechanism. These developments could enable low-cost QLED-based photomedical light sources with high brightness and outstanding color purity and pave the way for future display or lighting applications.

■ ASSOCIATED CONTENT

Supporting Information

The Supporting Information is available free of charge on the ACS Publications website at DOI: 10.1021/acs.jpclett.9b00499.

Details of SIH-QLED device fabrication, sample characterization and numerical simulation, description of the single LED with parasitic resistance model, note on a recent published paper, absorption and emission spectra of ZnO nanoparticles, absorption and emission spectra of as-synthesized QDs, L−J relationship for both devices, and performance comparison between different batches (PDF)

■ AUTHOR INFORMATION

Corresponding Authors

*D.Z.: E-mail: zhangdd@suda.edu.cn.
*S.-T.W.: E-mail: swu@ucf.edu.
*Y.D.: E-mail: Yajie.Dong@ucf.edu.

ORCID

Shin-Tson Wu: 0000-0002-0943-0440
Yajie Dong: 0000-0001-5319-2462

Author Contributions

⊥H.C. and Z.H. contributed equally. The manuscript was written through contributions of all authors. All authors have given approval to the final version of the manuscript.

Notes

The authors declare the following competing financial interest(s): Y. Dong is a cofounder of QLEDCures, LLC, which received an NSF STTR grant to develop quantum dot light-emitting diodes for photomedical applications.

■ ACKNOWLEDGMENTS

Y.D. thanks the American Society for Laser Medicine and Surgery, Inc. (ASLMS) and the Community Foundation of North Central Wisconsin for A. Ward Ford Memorial Research Grant support and the National Science Foundation for an STTR grant support (no. 1843101). D.Z. acknowledges the support of the National Natural Science Foundation of China (no. 61575134).

■ REFERENCES

(1) Shirasaki, Y.; Supran, G. J.; Bawendi, M. G.; Bulovic, V. Emergence of colloidal quantum-dot light-emitting technologies. *Nat. Photonics* **2013**, *7*, 13−23.
(2) Dai, X. L.; Deng, Y. Z.; Peng, X. G.; Jin, Y. Z. Quantum-Dot Light-Emitting Diodes for Large-Area Displays: Towards the Dawn of Commercialization. *Adv. Mater.* **2017**, *29*, 1607022.
(3) Lim, J.; Bae, W. K.; Kwak, J.; Lee, S.; Lee, C.; Char, K. Perspective on synthesis, device structures, and printing processes for quantum dot displays. *Opt. Mater. Express* **2012**, *2*, 594−628.
(4) Kathirgamanathan, P.; Bushby, L. M.; Kumaraverl, M.; Ravichandran, S.; Surendrakumar, S. Electroluminescent organic and quantum dot LEDs: The state of the art. *J. Disp. Technol.* **2015**, *11*, 480−493.
(5) Yang, Z.; Gao, M.; Wu, W.; Yang, X.; Sun, X. W.; Zhang, J.; Wang, H. C.; Liu, R. S.; Han, C. Y.; Yang, H.; Li, W. Recent advances in quantum dot-based light-emitting devices: Challenges and possible solutions. *Mater. Today* **2018**, DOI: 10.1016/j.mattod.2018.09.002.

DOI: 10.1021/acs.jpclett.9b00499
J. Phys. Chem. Lett. 2019, 10, 2196−2201

(6) Colvin, V. L.; Schlamp, M. C.; Alivisatos, A. P. Light-Emitting-Diodes Made from Cadmium Selenide Nanocrystals and a Semiconducting Polymer. *Nature* **1994**, *370*, 354−357.
(7) Mashford, B. S.; Stevenson, M.; Popovic, Z.; Hamilton, C.; Zhou, Z.; Breen, C.; Steckel, J.; Bulovic, V.; Bawendi, M.; Coe-Sullivan, S.; Kazlas, P. T. High-efficiency quantum-dot light-emitting devices with enhanced charge injection. *Nat. Photonics* **2013**, *7*, 407−412.
(8) Dong, Y.; Caruge, J. M.; Zhou, Z.; Hamilton, C.; Popovic, Z.; Ho, J.; Stevenson, M.; Liu, G.; Bulovic, V.; Bawendi, M.; Kazlas, P. T.; Steckel, J.; Coe-Sullivan, S. Ultra-Bright, Highly Efficient, Low Roll-Off Inverted Quantum-Dot Light Emitting Devices (QLEDs). *Dig. Tech. Pap. - Soc. Inf. Disp. Int. Symp.* **2015**, *46*, 270−273.
(9) Caruge, J. M.; Halpert, J. E.; Wood, V.; Bulovic, V.; Bawendi, M. G. Colloidal quantum-dot light-emitting diodes with metal-oxide charge transport layers. *Nat. Photonics* **2008**, *2*, 247−250.
(10) Dai, X.; Zhang, Z.; Jin, Y.; Niu, Y.; Cao, H.; Liang, X.; Chen, L.; Wang, J.; Peng, X. Solution-processed, high-performance light-emitting diodes based on quantum dots. *Nature* **2014**, *515*, 96−99.
(11) Yang, Y.; Zheng, Y.; Cao, W.; Titov, A.; Hyvonen, J.; Manders, J. R.; Xue, J.; Holloway, P. H.; Qian, L. High-efficiency light-emitting devices based on quantum dots with tailored nanostructures. *Nat. Photonics* **2015**, *9*, 259−266.
(12) Kwak, J.; Bae, W. K.; Lee, D.; Park, I.; Lim, J.; Park, M.; Cho, H.; Woo, H.; Yoon, D. Y.; Char, K.; Lee, S.; Lee, C. Bright and efficient full-color colloidal quantum dot light-emitting diodes using an inverted device structure. *Nano Lett.* **2012**, *12*, 2362−2366.
(13) Ghosh, B.; Yamada, H.; Chinnathambi, S.; Özbilgin, I. N. G.; Shirahata, N. Inverted Device Architecture for Enhanced Performance of Flexible Silicon Quantum Dot Light-Emitting Diode. *J. Phys. Chem. Lett.* **2018**, *9*, 5400−5407.
(14) Chen, B.; Pradhan, N.; Zhong, H. From Large-Scale Synthesis to Lighting Device Applications of Ternary I−III−VI Semiconductor Nanocrystals: Inspiring Greener Material Emitters. *J. Phys. Chem. Lett.* **2018**, *9*, 435−445.
(15) Wang, F.; Sun, W.; Liu, P.; Wang, Z.; Zhang, J.; Wei, J.; Li, Y.; Hayat, T.; Alsaedi, A.; Tan, Z. A. Achieving Balanced Charge Injection of Blue Quantum Dots Light-Emitting Diodes through Transport Layer Doping Strategies. *J. Phys. Chem. Lett.* **2019**, *10*, 960−965.
(16) Kamat, P. V.; Scholes, G. D. Quantum dots continue to shine brightly. *J. Phys. Chem. Lett.* **2016**, *7*, 584−585.
(17) Cao, W.; Xiang, C.; Yang, Y.; Chen, Q.; Chen, L.; Yan, X.; Qian, L. Highly stable QLEDs with improved hole injection via quantum dot structure tailoring. *Nat. Commun.* **2018**, *9*, 2608.
(18) *BOE Demonstrates Q-LED Display Prototypes*, 2017. https://www.oled-info.com/boe-demonstrates-q-led-display-prototypes (accessed 03/07/2019).
(19) Lin, Q.; Wang, L.; Li, Z.; Shen, H.; Guo, L.; Kuang, Y.; Wang, H.; Li, L. S. Nonblinking Quantum-Dot-Based Blue Light-Emitting Diodes with High Efficiency and a Balanced Charge-Injection Process. *ACS Photonics* **2018**, *5*, 939−946.
(20) Hamblin, M. R.; Huang, Y. *Handbook of Photomedicine*; Taylor & Francis: Boca Raton, FL, 2013.
(21) Chen, H.; He, J.; Lanzafame, R.; Stadler, I.; Hamidi, H. E.; Liu, H.; Celli, J.; Hamblin, M. R.; Huang, Y.; Oakley, E.; Shafirstein, G.; Chung, H. K.; Wu, S. T.; Dong, Y. Quantum dot light emitting devices for photomedical applications. *J. Soc. Inf. Disp.* **2017**, *25*, 177−184.
(22) Triana, M. A.; Chen, H.; Zhang, D.; Camargo, R. J.; Zhai, T.; Duhm, S.; Dong, Y. Bright inverted quantum-dot light-emitting diodes by all-solution processing. *J. Mater. Chem. C* **2018**, *6*, 7487−7492.
(23) Neyts, K. A. Simulation of light emission from thin-film microcavities. *J. Opt. Soc. Am. A* **1998**, *15*, 962−971.
(24) Yang, X.; Dev, K.; Wang, J.; Mutlugun, E.; Dang, C.; Zhao, Y.; Liu, S.; Tang, Y.; Tan, S. T.; Sun, X. W.; Demir, H. V. Light Extraction Efficiency Enhancement of Colloidal Quantum Dot Light-Emitting Diodes Using Large-Scale Nanopillar Arrays. *Adv. Funct. Mater.* **2014**, *24*, 5977−5984.
(25) Wang, S.; Dou, X.; Chen, L.; Fang, Y.; Wang, A.; Shen, H.; Du, Z. Enhanced light out-coupling efficiency of quantum dot light emitting diodes by nanoimprint lithography. *Nanoscale* **2018**, *10*, 11651−11656.
(26) Ni, X.; Kildishev, A. V.; Shalaev, V. M. Metasurface Holograms for Visible Light. *Nat. Commun.* **2013**, *4*, 2807.
(27) Ozaki, M.; Kato, J. I.; Kawata, S. Surface-Plasmon Holography with White-Light Illumination. *Science* **2011**, *332*, 218−220.
(28) Huang, L.; Chen, X.; Mühlenbernd, H.; Zhang, H.; Chen, S.; Bai, B.; Tan, Q.; Jin, G.; Cheah, K.-W.; Qiu, C.-W.; et al. Three-Dimensional Optical Holography Using a Plasmonic Metasurfaces. *Nat. Commun.* **2013**, *4*, 2808.
(29) Zheng, G.; Mühlenbernd, H.; Kenney, M.; Li, G.; Zentgraf, T.; Zhang, S. Metasurface Holograms Reaching 80% Efficiency. *Nat. Nanotechnol.* **2015**, *10*, 308−312.
(30) Pégard, N. C.; Fleischer, J. W. Optimizing Holographic Data Storage Using a Fractional Fourier Transform. *Opt. Lett.* **2011**, *36*, 2551−2553.
(31) Midgley, P. A.; Dunin-Borkowski, R. E. Electron Tomography and Holography in Materials Science. *Nat. Mater.* **2009**, *8*, 271−280.
(32) Dolev, I.; Epstein, I.; Arie, A. Surface-Plasmon Holographic Beam Shaping. *Phys. Rev. Lett.* **2012**, *109*, 203903.
(33) Zhou, L.; Ou, Q. D.; Shen, S.; Zhou, Y.; Fan, Y. Y.; Zhang, J.; Tang, J. X. Tailoring Directive Gain for High-Contrast, Wide-Viewing-Angle Organic Light-Emitting Diodes Using Speckle Image Holograpy Metasurfaces. *ACS Appl. Mater. Interfaces* **2016**, *8*, 22402−22409.
(34) Oh, J. Y.; Shin, M.; Lee, J. B.; Ahn, J. H.; Baik, H. K.; Jeong, U. Effect of PEDOT Nanofibril Networks on the Conductivity, Flexibility, and Coatability of PEDOT:PSS Films. *ACS Appl. Mater. Interfaces* **2014**, *6*, 6954−6961.
(35) Yoon, S. S.; Khang, D. Y. Roles of Nonionic Surfactant Additives in PEDOT:PSS Thin Films. *J. Phys. Chem. C* **2016**, *120*, 29525−29532.
(36) Shi, H.; Liu, C.; Jiang, Q.; Xu, J. Effective Approaches to Improve the Electrical Conductivity of PEDOT:PSS: A Review. *Adv. Electron. Mater.* **2015**, *1*, 1500017.
(37) Kim, T. H.; Cho, K. S.; Lee, E. K.; Lee, S. J.; Chae, J.; Kim, J. W.; Kim, D. H.; Kwon, J. Y.; Amaratunga, G.; Lee, S. Y.; Choi, B. L.; Kuk, Y.; Kim, J. M.; Kim, K. Full-colour quantum dot displays fabricated by transfer printing. *Nat. Photonics* **2011**, *5*, 176−182.
(38) Jayam, S. G.; Navaneethakrishnan, K. Effects of electric field and hydrostatic pressure on donor binding energies in a spherical quantum dot. *Solid State Commun.* **2003**, *126*, 681−685.

DOI: 10.1021/acs.jpclett.9b00499
J. Phys. Chem. Lett. 2019, 10, 2196−2201